Available online at www.sciencedirect.com
SCIENCE DIRECT
Journal of Catalysis 241 (2006) 200–210
JOURNAL OF CATALYSIS
www.elsevier.com/locate/jcat

In situ FTIR study of SO_2 interaction with $Pt/BaCO_3/Al_2O_3$ NO_x storage catalysts under lean and rich conditions

Hussam Abdulhamid [a,b,*], Erik Fridell [a,c,1], Jazaer Dawody [a,c], Magnus Skoglundh [a,b]

[a] *Competence Centre for Catalysis, Chalmers University of Technology, SE-412 96 Göteborg, Sweden*
[b] *Department of Chemical and Biological Engineering – Applied Surface Chemistry, Chalmers University of Technology, SE-412 96 Göteborg, Sweden*
[c] *Department of Applied Physics, Chalmers University of Technology, SE-412 96 Göteborg, Sweden*

Received 7 March 2006; revised 24 April 2006; accepted 30 April 2006

Abstract

The interaction of SO_2 with $Pt/BaCO_3/Al_2O_3$ NO_x storage catalysts under lean and rich conditions in the absence and presence of water was investigated by means of in situ FTIR spectroscopy at 350 °C. For the lean condition ($SO_2 + O_2$), surface and bulk barium sulfates were formed in addition to sulfites and surface sulfates on alumina. Pt does not appear to play an essential role in the formation of these species under lean conditions. In contrast, under reducing conditions ($SO_2 + H_2$), Pt catalysed the reduction of SO_2 with H_2 to form reduced sulfur species that accumulate on both Pt and barium sites. A subsequent treatment with NO_2 resulted in the reduction of NO_2 in the oxidation of these sulfur-containing species to form bulk barium sulfate instead of being stored over barium sites. Introducing water significantly affected sulfur trapping over the catalyst surface. During the lean conditions, the presence of water resulted in almost no surface barium sulfate formation. Meanwhile, the formation of bulk barium sulfate was increased, probably due to enhanced sulfate formation. However, the presence of H_2O under reducing conditions resulted in significantly lower sulfur storage on both barium and alumina in comparison with humid lean exposure conditions.

Keywords: NO_x storage catalyst; $Pt/BaCO_3/Al_2O_3$ catalyst; Lean NO_2 reduction; DRIFT; Sulfur poisoning; SO_2, H_2O

1. Introduction

Lean-burn gasoline and diesel engines provide good fuel economy and relatively low CO_2 emissions. However, the reduction of nitrogen oxides (NO_x) to nitrogen is strongly limited due to the high oxygen concentration in the exhausts of such engines. NO_x storage is a promising technology for overcoming this problem, where the emitted NO_x during the lean period is stored on a specific storage component in the catalyst until saturation and then regenerated in a short rich period when the stored NO_x is released and reduced to N_2 [1].

One main disadvantages with the NO_x storage concept is the loss of NO_x storage capacity in the presence of even very small amounts of sulfur in the exhausts [2]. Sulfur oxides interact with the storage component (typically barium oxide or barium carbonate) and the support (usually alumina) during the lean phase. During the rich period, mainly NO_x desorbs from the catalyst due to the higher stability of sulfates compared with nitrates. Sulfur species thus accumulate in the catalyst, significantly reducting NO_x storage capacity [3]. Substantial studies have been performed to investigate sulfur deactivation in the NO_x storage process. One key tool that can be used in this connection is the in situ Fourier transform infrared spectroscopy (FTIR), which makes it possible to identify and follow the evolution of surface species under different conditions, providing essential information on the deactivation process [4].

In the literature, FTIR and flow reactor studies have been used to examine and understand the sulfur deactivation process over NO_x storage catalysts. The main findings from these studies can be summarised as follows:

– Sulfur, as SO_2, H_2S, or COS, causes deactivation of storage components as well as precious metals. It accumulates over

* Corresponding author. Fax: +46 31 160062.
E-mail address: husam@chem.chalmers.se (H. Abdulhamid).
[1] Present address: IVL Swedish Environmental Research Institute, PO Box 5302, SE-411 33 Göteborg, Sweden.

0021-9517/$ – see front matter
doi:10.1016/j.jcat.2006.04.034

alumina as sulfite, surface sulfate (after being oxidised over the precious metal) [5], and probably as bulk sulfate [6] and over barium as both surface and bulk sulfate [5,7]. Formation of sulfides over the precious metal sites (Pt) during the reduction period blocks these sites, leading to deterioration in the regeneration process [8,9].
- Hydrogen can regenerate sulfur-deactivated samples more efficiently than carbon monoxide [10].
- Sulfate formation proceeds more slowly than nitrate formation; however, the sulfates are more stable than the nitrates [11].
- Thermodynamic calculations show that in the presence of H_2, the decomposition of $BaSO_4$ to BaO with H_2S as a reaction product can occur at temperatures significantly lower than those required for the corresponding decomposition to BaO with SO_2 as a reaction product [12].
- Both H_2O and CO_2 significantly affect the NO_x regeneration process of sulfated NO_x storage catalysts [5,13]. Thermodynamic calculations reveal that in the presence of CO_2 under H_2-rich conditions, formation of $BaCO_3$ is thermodynamically more feasible than formation of BaO at lower temperatures [12]. On the other hand, H_2O has shown the ability to enhance the sorption of sulfur over alumina [14,15].
- Different types of precious metals have different impacts on the sulfur deactivation and regeneration processes [16].
- Additives can be used to increase the sulfur tolerance of barium-based NO_x storage catalyst. Generally, higher sulfur tolerance is related to either lower sulfate decomposition temperature [12,17] or formation of high sulfur-resistance metal phases [18].

It has been shown previously [9,19,20] that the NO_x storage capacity of barium-based catalysts decays faster during rich SO_2 exposure conditions than in lean SO_2 exposure conditions. This faster deactivation during rich exposure conditions has been related to the accumulation of sulfur-containing species on the noble metal sites, resulting in deterioration of the noble metal activity for reduction. However, the pathways for the formation and accumulation of the different sulfur-containing species on the noble metal and the storage sites have not been shown. Thus, a detailed investigation of the interaction between sulfur and the different washcoat components may provide a deeper understanding of the sulfur deactivation process.

In the current investigation, in situ DRIFTS was used to follow the evolution of different surface species (as well as any probable intermediates) during SO_2 exposure to a $Pt/BaCO_3/Al_2O_3$ catalyst under lean and rich conditions in the presence and absence of water. Moreover, to understand the role of each of the washcoat components (i.e., Pt, Ba, and Al_2O_3) in the deactivation process and more accurately interpret the formation of different surface species, the same experiments were also performed for samples with individual components, that is, $BaCO_3/Al_2O_3$, Pt/Al_2O_3, and Al_2O_3.

2. Experimental

2.1. Catalyst preparation and characterisation

Four different powder samples based on Pt, Ba, and Al_2O_3 were prepared: $Pt/BaCO_3/Al_2O_3$, $BaCO_3/Al_2O_3$, Pt/Al_2O_3, and Al_2O_3. To prepare the $BaCO_3/Al_2O_3$ sample, an aqueous solution of $Ba(NO_3)_2$ was added to γ-Al_2O_3 (SBa-200 from Sasol) dispersed in Milli-Q water under continuous stirring, and the pH of the solution was adjusted to 11 by adding NH_4OH. The sample was then freeze-dried and calcined in air at 600 °C for 1 h. An aqueous solution of ammonium carbamate was then added under continuous stirring to the barium–alumina sample to accomplish the formation of barium carbonate. The sample was finally freeze-dried and calcined in air at 500 °C for 1 h. The final $BaCO_3$ loading of the $BaCO_3/Al_2O_3$ sample was 20 wt%.

The $Pt/BaCO_3/Al_2O_3$ sample was prepared by adding an aqueous solution of $Pt(NO_3)_2$ to a fraction of the $BaCO_3/Al_2O_3$ sample dispersed in Milli-Q water under continuous stirring for 1 h. The sample was then freeze-dried and calcined in air at 550 °C for 2 h. The final Pt loading of the sample was 2 wt% of the total washcoat.

The Pt/Al_2O_3 sample was prepared by adding a platinum nitrate solution (containing an amount of platinum corresponding to 2 wt% of the total washcoat) to γ-Al_2O_3 dispersed in Milli-Q water under continuous stirring for 1 h. The sample was then freeze-dried and calcined in air at 550 °C for 2 h.

Finally, the powder Al_2O_3 used in DRIFTS experiments was prepared by calcining γ-Al_2O_3 for 2 h at 550 °C.

The specific surface area of the different powder samples was determined by nitrogen adsorption according to the BET method using a TriStar 3000 instrument (Micrometrics).

The noble metal dispersion for the two Pt-containing catalysts was determined using the N_2O dissociation method described elsewhere [21] after supporting 250 mg of each powder sample on monolith substrates. The substrates were immersed in a slurry (prepared by 20 wt% colloidal silica [Nyacol 2034DI, Akzo Nobel] and the powder sample, dispersed in distilled water) until the channels were filled. The samples were then dried at 95 °C for 2 h. The procedure was repeated until the desired amount of washcoat was deposited on the monolith substrates. Finally, the samples were calcined in air at 550 °C for 1 h. The results from the Pt-dispersion and BET surface area measurements of the samples are presented in Table 1.

Table 1
Compositions, BET surface area, and estimated noble metal dispersion

Powder catalysts	Pt (wt%)	$BaCO_3$ (wt%)	Al_2O_3 (wt%)	BET (m^2/g)	Metal dispersion[a] (%)
$Pt/BaCO_3/Al_2O_3$	2.0	20	78	161	5
$BaCO_3/Al_2O_3$	–	20	80	186	–
Pt/Al_2O_3	2.0	–	98	187	23
Al_2O_3	–	–	100	200	–

[a] The noble metal dispersion was calculated for the powder samples supported on monolith substrates.

2.2. DRIFTS experiments

The formation and evolution of both surface and bulk species during SO_2 exposure under both oxidising and reducing conditions were investigated in situ using a BioRad FTS6000 FTIR spectrometer equipped with a heated reaction chamber (Harrick Scientific Praying Mantis DRIFTS cell with KBr windows) and a resolution of 2 cm^{-1}. All experiments were conducted at a constant temperature of 350 °C, at which maximum NO_x storage performance was achieved, and a total flow rate of 150 ml/min, corresponding to a space velocity of 79,500 h^{-1}. The space velocity in the DRIFTS cell was calculated by dividing the total flow with the catalyst volume. The catalyst volume was assumed to be equal to the volume of the filled powder sample holder inside the cell.

Before all experiments, each sample (about 150 mg) was preoxidised at 450 °C in 8% O_2 in Ar for 10 min, flushed with Ar for 5 min, and prereduced in 2% H_2 in Ar for 10 min. The sample was then exposed to Ar, and the temperature was lowered to 350 °C and kept constant for 5 min. Then the experiments under different exposure conditions were performed with the setups described in the following sections.

2.2.1. SO_2 exposure under lean and rich conditions

The sulfur DRIFTS experiments under oxidising and reducing conditions were conducted by exposing the pretreated sample either to 8% O_2 in Ar (for oxidation) or 2% H_2 in Ar (for reduction) for 5 min as the background spectrum was collected. Then 100 ppm SO_2 was introduced to the sample cell, and spectra were collected once every min for 30 min to follow the evolution of different surface species.

2.2.2. SO_2 exposure in presence of water

To study the effect of water on the formation of different sulfur species, water vapour was added to the reactant feed by passing 50 ml/min of Ar as a carrying gas through an insulated stainless steel bottle filled with distilled water at 45 °C. This feed was mixed with the main gas feed before entering the DRIFTS cell, resulting in a water vapor content of 3% with a constant total flow rate of 150 ml/min.

The DRIFTS experiments were conducted by introducing 3% water with either 8% O_2 in Ar (for oxidation) or 2% H_2 in Ar (for reduction) for 5 min before the background spectrum was collected. Then 100 ppm SO_2 was introduced into the gas mixture and spectra were collected once every min for a time duration of 30 min.

3. Results and discussion

3.1. Exposure of SO_2 under oxidising conditions

Fig. 1 shows the in situ DRIFTS spectra during exposure of 100 ppm SO_2 and 8% O_2 to the Pt/Ba CO_3/Al_2O_3 catalyst at 350 °C for 30 min. It is obvious that at the beginning of the experiment, peaks grew predominantly in the 1400–900 cm^{-1} region with maxima at 1318, 1249, 1168, 1107, and 972 cm^{-1}. These peaks can be assigned to different sulfite and sulfate species.

The 1107 cm^{-1} peak is assigned to S–O vibration for surface barium sulfate [7,8] whereas the bands at 1249 and 1168 cm^{-1} are assigned to S=O and S–O vibrations for bulk barium sulfate [7,8,22]. Furthermore, the peak at 972 cm^{-1} in addition to two broad bands at 3638 and 3570 cm^{-1} (not shown) most likely can be attributed to hydrogen-bonded sulfites on alumina [15], whereas the peak at 1318 cm^{-1} is assigned to surface aluminum sulfate. In addition to the formation of different surface sulfite and sulfate species, negative peaks at 1581, 1496 and 1456 cm^{-1} appear as a result of the replacement of surface and bulk barium carbonate with their corresponding sulfate species.

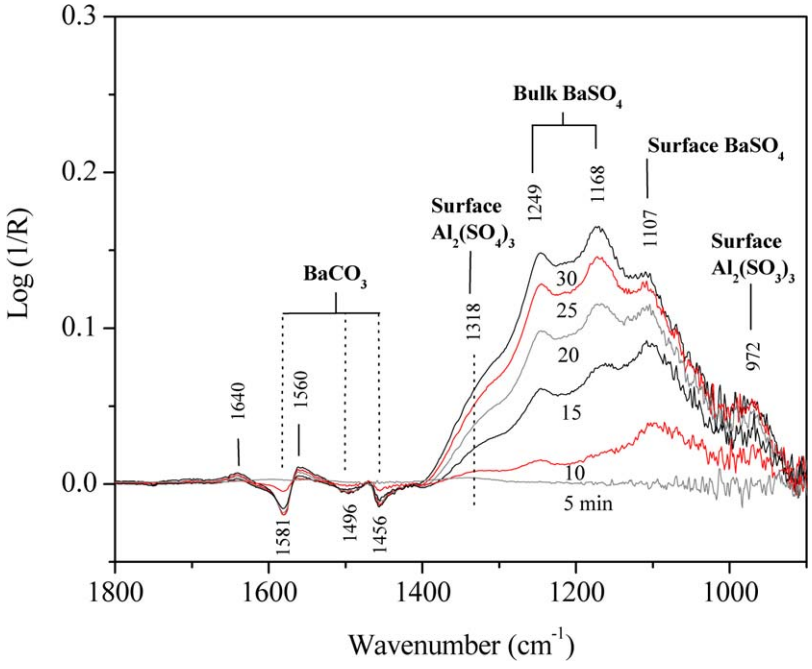

Fig. 1. DRIFT spectra for the Pt/$BaCO_3$/Al_2O_3 sample after exposure to 100 ppm SO_2 and 8% O_2 in Ar at 350 °C for 5, 10, 15, 20, 25 and 30 min.

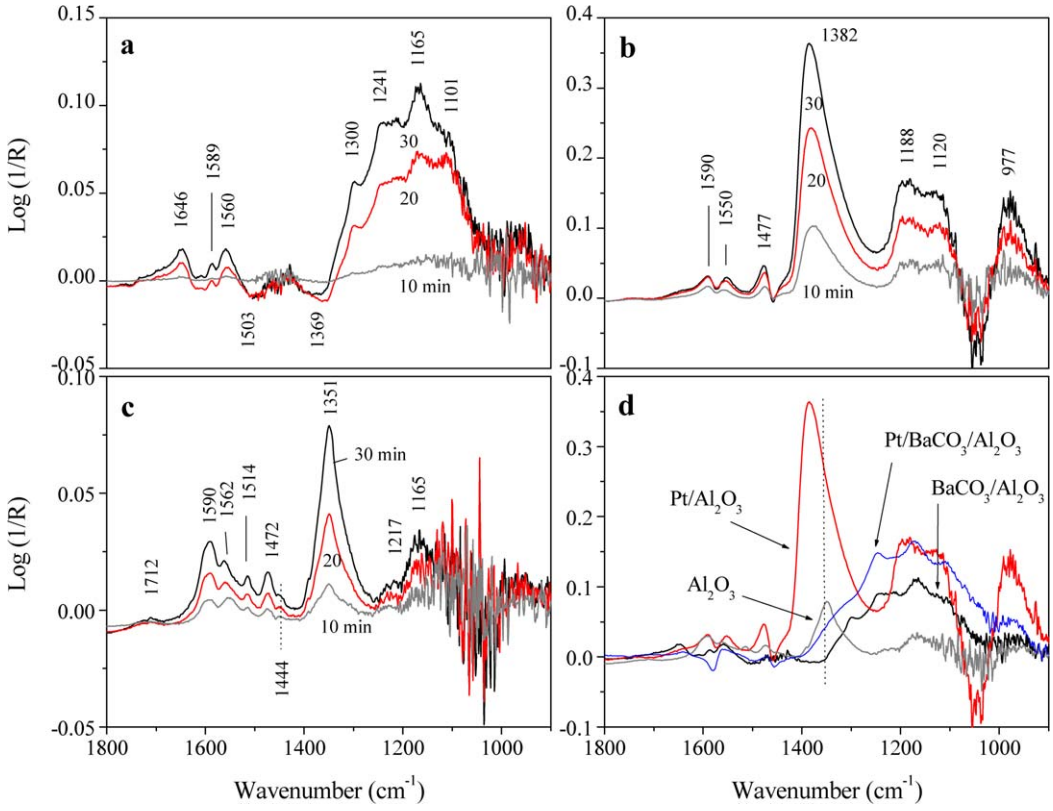

Fig. 2. DRIFT spectra for (a) $BaCO_3/Al_2O_3$, (b) Pt/Al_2O_3, and (c) Al_2O_3 samples after exposure to 100 ppm SO_2 and 8% O_2 in Ar at 350 °C for 10, 20 and 30 min. (d) DRIFT spectra for the $Pt/BaCO_3/Al_2O_3$ sample and the $BaCO_3/Al_2O_3$, Pt/Al_2O_3 and Al_2O_3 samples after 30 min exposure to 100 ppm SO_2 and 8% O_2 in Ar at 350 °C.

Negative peaks at 3751 and 3720 cm^{-1} (not shown) result from the interaction of SO_2 with surface OH groups on alumina [23].

The same experiment was performed for the $BaCO_3/Al_2O_3$, Pt/Al_2O_3 and Al_2O_3 samples at 350 °C. The DRIFTS spectra for these samples are shown in Fig. 2. For the $BaCO_3/Al_2O_3$ sample, the main features during $SO_2 + O_2$ exposure (Fig. 2a) are related to surface and bulk barium sulfates (bands at 1101, 1165, and 1241 cm^{-1}, respectively) in addition to surface aluminum sulfate (1300 cm^{-1}). The spectra also show a progressive growth of negative peaks at 1503 and 1369 cm^{-1} related to the decomposition of barium carbonate.

In a previous investigation by Dawody et al. [19], $BaCO_3/Al_2O_3$ was alternately exposed in a flow reactor to 630 ppm $NO_2 + 8\%$ O_2 and 40 ppm $SO_2 + 8\%$ O_2 at 300 °C to study the effect of sulfur exposure condition on the NO_x storage performance. It was shown that almost no sulfur was trapped in the $BaCO_3/Al_2O_3$ sample, and it was concluded that only weakly adsorbed sulfur species were formed as a consequence of the absence of precious metal in the sample. To clarify whether exposure to NO_x before exposure to SO_2 affects the adsorption of SO_x, a fresh $BaCO_3/Al_2O_3$ sample was exposed to 500 ppm NO_2 in Ar, followed by a temperature ramp before the $SO_2 + O_2$ exposure. The results show that the sample still adsorbed sulfur as surface and bulk barium sulfates. Thus, the discrepancy between the current results and the results in the work of Dawody et al. [19] is probably due to differences in such parameters as SO_2 concentration, temperature, and space velocity.

The spectra for the SO_2 oxidation experiment over the Pt/Al_2O_3 sample (Fig. 2b) reveal a significant increase in the intensity of adsorbed surface sulfur species on alumina with dominant peaks at 1382, 1188, 1120 and 977 cm^{-1}. These peaks have been attributed to surface aluminum sulfate (1381 cm^{-1}) [11], either bulk aluminum sulfate [11] or surface adsorbed SO_2 (1188 cm^{-1}) [24], surface aluminum sulfate (1120 cm^{-1}) [5], and sulfite over alumina (977 cm^{-1}) [15], respectively.

The corresponding spectra for Al_2O_3 during SO_2 exposure in presence of O_2 are shown in Fig. 2c. The intense band at 1351 cm^{-1} can be attributed to surface aluminum sulfate, and the bands at 1217 with 1165 cm^{-1} can be assigned to bulk sulfate species [7,25].

From Fig. 1, it is clear that when exposing the $Pt/BaCO_3/Al_2O_3$ sample to SO_2 under oxidising conditions, surface barium sulfates (1107 cm^{-1}) are formed in addition to smaller amounts of bulk barium sulfates (bands at 1168 and 1249 cm^{-1}) at the beginning of the SO_2 exposure. However, with time (continuous $SO_2 + O_2$ exposure), the intensity of the surface barium sulfate peaks becomes less than the intensity of bulk barium sulfate peaks, indicating the conversion of surface sulfates to bulk sulfates of barium, in line with the findings by Sedlmair et al. [8]. The assignment of the 1107, 1168 and 1249 cm^{-1} bands to surface and bulk barium sulfate rather than to alumina-bonded sulfates is supported by the fact that these bands were

observed only for the barium-containing samples (see Fig. 2d). Moreover, the formation of these species is relatively independent of the presence of Pt, because they clearly exist on the Pt-free sample (Fig. 2a), albeit at lower intensity. Su and Amiridis [7] investigated the $SO_2 + O_2$ exposure to a similar catalyst system and found that the formation of surface barium sulfates was independent of the presence of Pt under lean conditions. In addition, for an alumina sample, only the adsorption of SO_2 was observed under such conditions through the formation of surface aluminum sulfate (1318 cm^{-1}) and sulfite (972 cm^{-1}). According to Saur et al. [26], surface aluminum sulfate is characterised by two peaks at around 1380 and 1035 cm^{-1} for S=O and S–O stretching vibrations, respectively. However, we could not observe the 1035 cm^{-1} peak and thus believe that these frequencies (1380 and 1035 cm^{-1}) are related to different species, in agreement with Chang and Uy et al. [11,14] who assigned the 1035 cm^{-1} peak to a bulk-like from of sulfate. The formation of aluminum sulfite was obviously catalysed by the presence of platinum. Fig. 2d shows a clear maximum at 977 cm^{-1} for the Pt/Al_2O_3 sample only, which is due to the formation of aluminum sulfite.

As discussed previously, the bands at 3638 and 3570 cm^{-1} are assigned to the interaction of SO_2 with alumina. This interaction may induce changes in the OH stretching vibration resulting from the formation of hydrogen-bonded sulfite species. However, formation of bands at these wavenumbers was also observed for samples in which no sulfites were adsorbed (Fig. 2d), and thus the surface aluminum sulfates likely also are bonded to the hydrogen of alumina OH– groups, causing the same effect on the OH vibration frequency. Furthermore, during exposure to $SO_2 + O_2$, all samples develop adsorption peaks between 1720 and 1450 cm^{-1}. These peaks may be a result of barium carbonate displacement by sulfates and can be attributed to surface carbon containing species [11] adsorbed on alumina and barium. The peaks in the 1400–1600 cm^{-1} region are likely due to adsorption of different species over alumina, whereas the peak around 1640 cm^{-1} more likely can be attributed to species adsorbed on barium, because this peak appears only on the barium-containing samples. However, the latter peak also may be due to the adsorption of small amounts of surface-bonded water resulting from the release of OH groups from the alumina surface, where water shows a bending frequency at around 1630 cm^{-1} [27].

3.2. Exposure to SO_2 under reducing conditions

Fig. 3 shows the in situ DRIFTS spectra for the $Pt/BaCO_3/Al_2O_3$ sample during exposure to 100 ppm SO_2 and 2% H_2 in Ar at 350 °C. Adsorption bands that increase continuously during $SO_2 + H_2$ exposure are observed at 1230 with 1157, 1103 and 987 cm^{-1}. These bands are assigned to bulk and surface barium sulfate and aluminum sulfite, respectively. In addition, negative peaks observed at 1542 and 1376 cm^{-1} are probably due to barium carbonate displacement. Furthermore, a broad negative band is observed between 2070 and 1800 cm^{-1} with a maximum at 2041 cm^{-1}. We believe that this feature corresponds to the removal of linear- and bridge-bonded CO over platinum [28,29], where CO adsorption on Pt is seen in the background spectrum taken in H_2/Ar atmosphere (see the inset in Fig. 3). The formation of CO during the H_2/Ar pretreatment is suggested to take place according to

$$BaCO_3 + H_2 \rightarrow BaO + CO + H_2O \quad (1)$$

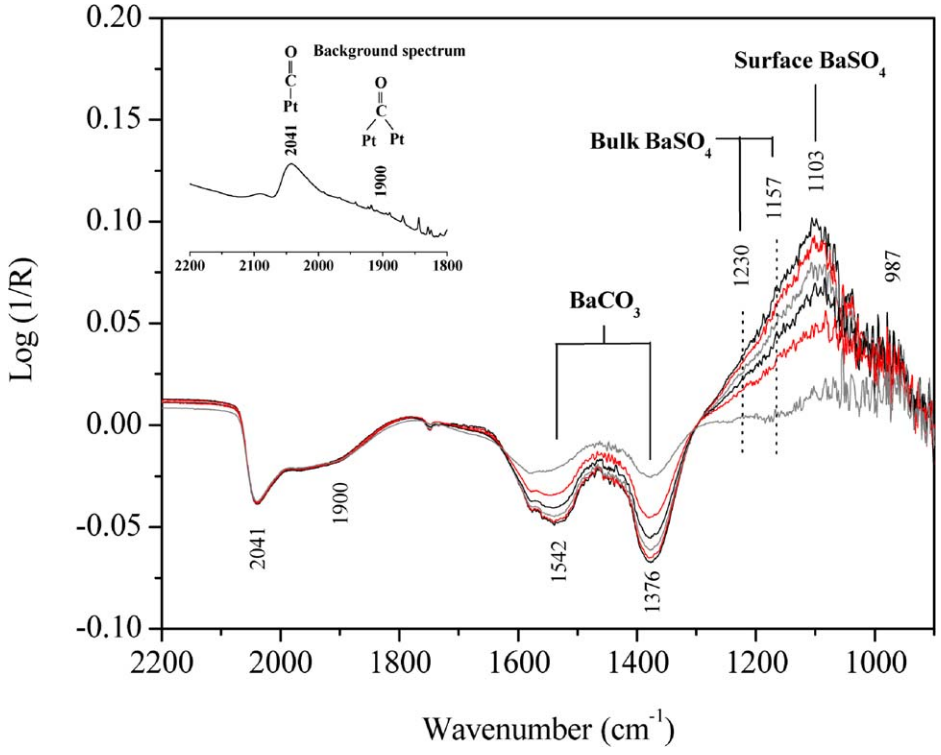

Fig. 3. DRIFT spectra for the $Pt/BaCO_3/Al_2O_3$ sample after exposure to 100 ppm SO_2 and 2% H_2 in Ar at 350 °C for 5, 10, 15, 20, 25 and 30 min.

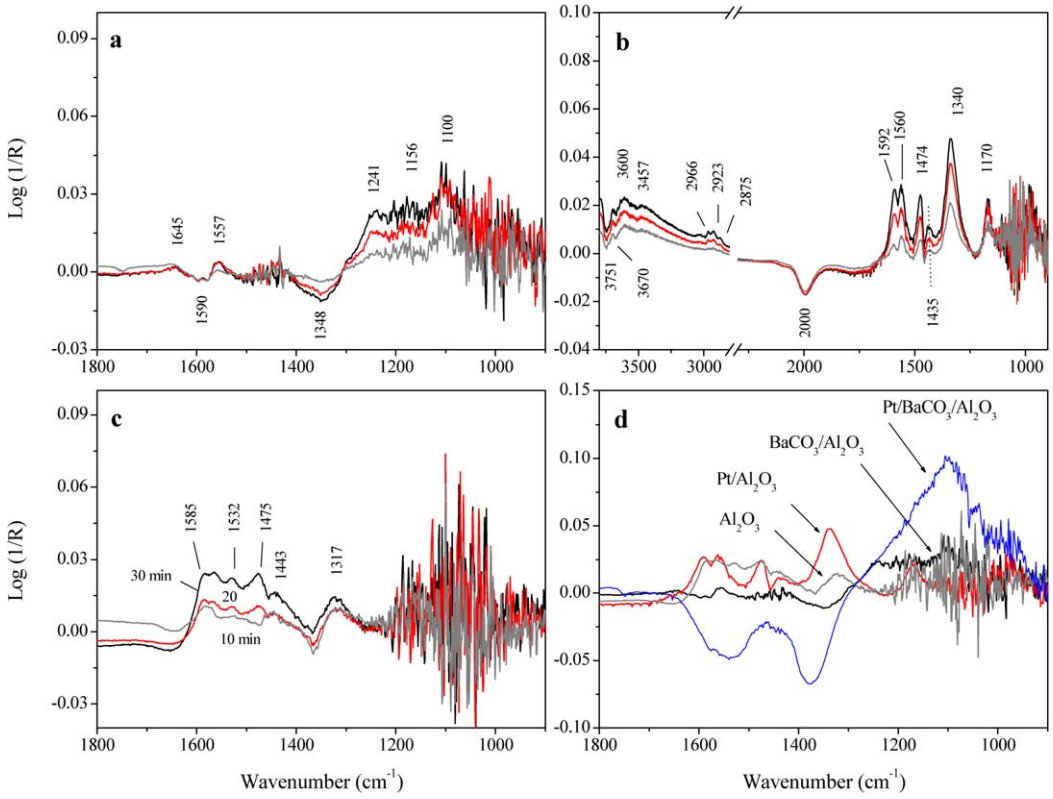

Fig. 4. DRIFT spectra for (a) $BaCO_3/Al_2O_3$, (b) Pt/Al_2O_3, and (c) Al_2O_3 samples at 350 °C after exposure to 100 ppm SO_2 and 2% H_2 in Ar for 10, 20 and 30 min. (d) DRIFT spectra for the $Pt/BaCO_3/Al_2O_3$ sample and the $BaCO_3/Al_2O_3$, Pt/Al_2O_3 and Al_2O_3 samples after 30 min exposure to 100 ppm SO_2 and 2% H_2 in Ar at 350 °C.

or

$$BaCO_3 + H_2 \rightarrow Ba(OH)_2 + CO. \quad (2)$$

The relatively high intensity of the negative peaks for CO adsorbed over platinum could be explained by the characteristic strong IR absorption for CO. Negative peaks observed at 3751, 3719, and 3665 cm^{-1} (not show in Fig. 3) represent the interaction between surface hydroxyl groups on alumina and SO_2.

Fig. 4a shows the IR spectra for the $BaCO_3/Al_2O_3$ sample during SO_2 exposure in presence of H_2. Compared with the $Pt/BaCO_3/Al_2O_3$ sample, less surface and bulk barium sulfates for this sample are observed, as indicated by the lower intensity of the bands at 1100, 1156, and 1241 cm^{-1} together with the lower intensity of the negative bands related to decomposition of barium carbonate at 1348 and 1590 cm^{-1}.

The main features observed for the Pt/Al_2O_3 sample on exposure to $SO_2 + H_2$ (Fig. 4b) are the formation of surface aluminum sulfate and either bulk aluminum sulfate or surface adsorbed SO_2 with bands at 1340 and 1170 cm^{-1}, respectively. In addition, peaks are observed at 1996, 2923 and 2875 cm^{-1}, which probably can be related to hydrogen–carbon containing species [30], as a result of carbon release from the alumina in the presence of hydrogen.

For the Al_2O_3 sample (Fig. 4c), surface aluminum sulfate at 1317 cm^{-1} is observed. The intensity of this peak is much lower than that of the corresponding peak in the Pt/Al_2O_3 sample.

The exposure of the $Pt/BaCO_3/Al_2O_3$ sample to SO_2 under reducing conditions results in the formation of considerable less surface and bulk sulfate species (peaks at 1103, 1157, and 1230 cm^{-1}) compared with SO_2 exposure under oxidising conditions. Furthermore, $SO_2 + H_2$ exposure results in the formation of aluminum sulfite, whereas clearly no surface aluminum sulfate could be identified. For the Pt/Al_2O_3 and Al_2O_3 samples, the intensity of the surface aluminum sulfate peak is low, indicating that only small amounts are formed. This in turn means that the formation of aluminum sulfate on the $Pt/BaCO_3/Al_2O_3$ catalyst under these conditions is even lower, due to partial coverage of the Al_2O_3 surface with barium.

The formation of less surface barium sulfates during SO_2 exposure under rich conditions in comparison to lean SO_2 exposure can most likely be related to the limitation in the formation of sulfates as a consequence of O_2 deficiency under reducing conditions. A possible pathway for the low sulfate formation during reducing conditions may be related to the presence of some oxygen resulting from the dissociation of SO_2 over the precious metal. This may explain the pronounced difference in surface barium sulfate formation between the $Pt/BaCO_3/Al_2O_3$ and $BaCO_3/Al_2O_3$ samples shown in Fig. 4d.

3.2.1. *Effect of $SO_2 + H_2$ exposure on the NO_x storage performance of $Pt/BaCO_3/Al_2O_3$*

A more interesting observation for the $Pt/BaCO_3/Al_2O_3$ sample (Fig. 3) is the much lower intensity of the peaks corresponding to bulk barium sulfate (peaks at 1230 and 1157 cm^{-1}) compared with sulfur exposure under oxidation conditions (Fig. 1). Before explaining this low formation, we note that the sample was reduced with H_2 for 5 min before the SO_2 was introduced under continuous hydrogen supply. Thus, surface

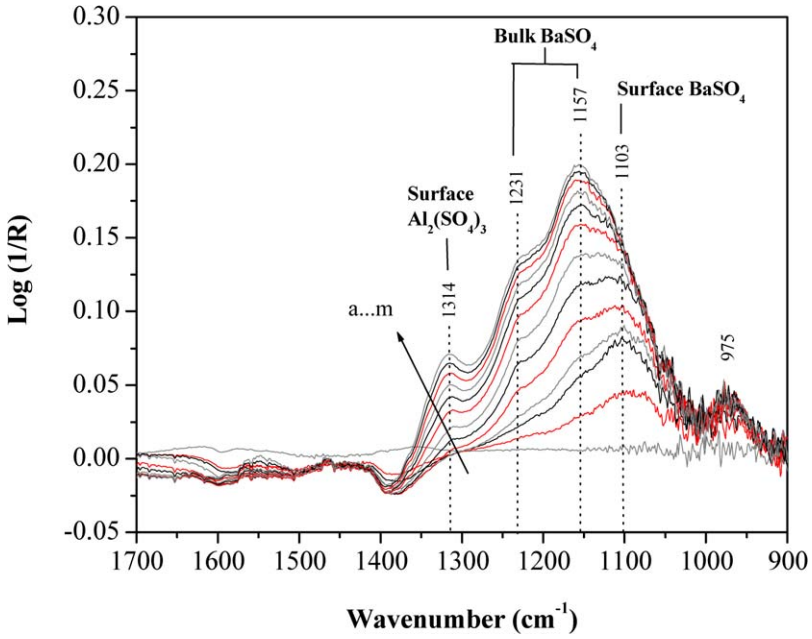

Fig. 5. DRIFT spectra for the $Pt/BaCO_3/Al_2O_3$ sample 350 °C after exposure to 100 ppm SO_2 and 2% H_2 in Ar at 350 °C for (a) 10, (b) 20, and (c) 30 min; followed by 10 min oxidation in 500 ppm NO_2 in Ar. Spectra (d)–(m) collected after each min of NO_2 exposure.

barium carbonate as well as part of the bulk barium carbonate is expected to be in form of barium oxide or barium hydroxide, according to reactions (1) and (2).

The observed low formation of bulk barium sulfate might be explained by the interaction of BaO and/or $Ba(OH)_2$ with reduced sulfur-containing species formed from the reaction of SO_2 with H_2 over platinum sites. Elbouazzaoui et al. [31] and Poulston and Rajaram [13] used XRD to characterise barium-based samples after exposure to $SO_2 + H_2$ and observed the formation of BaS. Eysel et al. [32] assigned a band at 473 cm^{-1} to the vibrational frequency for Ba–S. However, because the detection of species with vibrational frequencies below about 1000 cm^{-1} is strongly limited with the FTIR equipment used in the current study, we could not experimentally verify formation of barium sulfide. In the current work we could not observe any H_2S adsorption on the surface during $SO_2 + H_2$ exposure, which should give a S–H stretching vibration at around 2663 cm^{-1} and bending vibrations at 2539 and 1360 cm^{-1} [33,34]. Thus, the formation of H_2S observed in different gas-phase studies [10,19,31] is expected to be a rather fast reaction step.

To study the NO_2 interaction with the $Pt/BaCO_3/Al_2O_3$ sample that had been exposed to $SO_2 + H_2$, the catalyst was subsequently (after $SO_2 + H_2$ treatment) and in situ exposed to 500 ppm NO_2 in Ar for 20 min, with the expectation of oxidation of the accumulated reduced sulfur species over barium sites to sulfates. The expected formation of surface and bulk sulfates was observed immediately after starting the NO_2, as shown in Fig. 5. For clarity, only the first 10 min of NO_2 exposure is shown in the figure, to prevent the overlapping of bulk barium sulfates and surface aluminum sulfates with the nitrite/nitrate peaks appearing in the range of about 1600–1230 cm^{-1} [18,35,36]. As shown in Fig. 5, the peaks for surface and bulk barium sulfates in addition to surface aluminum sulfates are growing with NO_2 exposure time. This strongly suggests that the deactivation of the NO_x storage performance of the sample on SO_2 exposure under rich conditions is due to formation of sulfides that obstruct the NO_2 storage function. These sulfides are oxidised by NO_2 to barium sulfides, whereby NO_2 is reduced to NO rather than being stored as barium nitrites and nitrates. This can explain the greater decrease in NO_x storage capacity for this type of sample when exposed to sulfur under reducing conditions compared with oxidising conditions, as reported by Amberntsson et al. [16] and Dawody et al. [19].

An interesting feature in Fig. 5 is the growth of the peak at 1314 cm^{-1} related to surface aluminum sulfate, in a similar manner as the growth of peaks related to surface and bulk barium sulfate after exposure of the $SO_2 + H_2$-treated $Pt/BaCO_3/Al_2O_3$ sample to NO_2. This suggests that exposure to $SO_2 + H_2$ results in the accumulation of reduced surface species on alumina as it does for barium.

The reduced sulfur species can interact either with all barium sites or mainly with barium sites in the platinum–barium interface. Fig. 6 shows the spectra for the $SO_2 + H_2$-treated $Pt/BaCO_3/Al_2O_3$ sample after exposure to NO_2 for 10 min (spectra a) and 20 min (spectra b) at 350 °C. It is interesting that during the first 10 min of NO_2 exposure, no nitrite/nitrate peaks formed over the catalyst surface. After NO_2 exposure, the sample was followed by thermal treatment in Ar to 520 °C (spectra b–e). It is clear from the figure that even though the temperature is increased to 520 °C, the nitrite and nitrate peaks are still present (represented by the peaks at 1548 cm^{-1} [7] on alumina and at 1328 and 1303 cm^{-1} on barium [8,18]). This may indicate that the NO_x storage in $SO_2 + H_2$-treated $Pt/BaCO_3/Al_2O_3$ may occur over storage sites far away from the Pt sites, and thus the NO_x desorption profile shifts toward higher temperatures, similar to platinum-free barium-based samples [37]. This

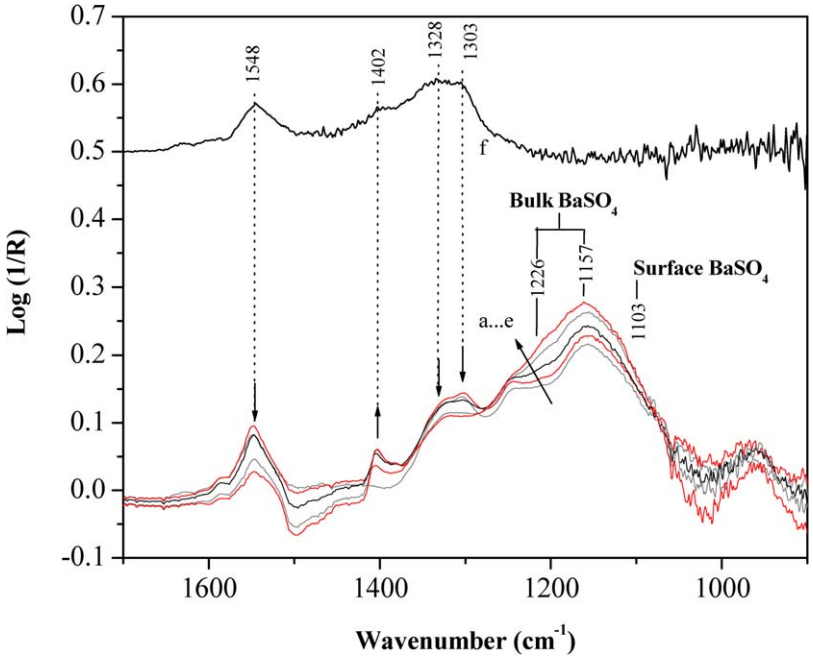

Fig. 6. DRIFT spectra for the $Pt/BaCO_3/Al_2O_3$ sample exposed to $SO_2 + H_2$ followed by exposure to (a) 500 ppm NO_2 for 20 min at 350 °C, (b) flushed with Ar at 400 °C, (c) 450 °C, (d) 500 °C, and (e) 520 °C. (f) DRIFT spectra for a fresh $Pt/BaCO_3/Al_2O_3$ sample exposed to 500 ppm NO_2 in Ar for 18 min at 350 °C.

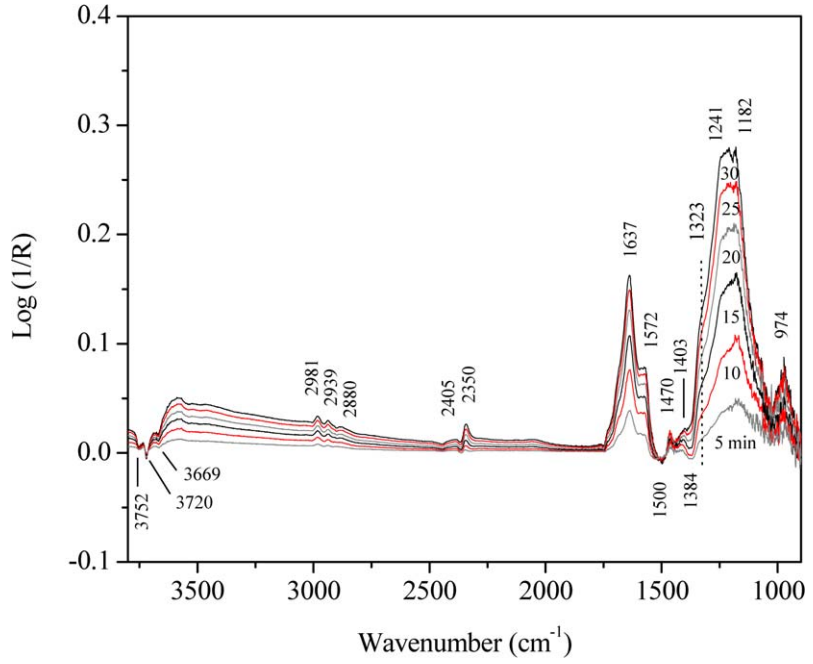

Fig. 7. DRIFT spectra for the $Pt/BaO/Al_2O_3$ sample after exposure to 100 ppm SO_2, 8% O_2 and 3% H_2O in Ar at 350 °C for 5, 10, 15, 20, 25 and 30 min.

may provide evidence that the sulfur deactivation initially occurs on storage sites close to platinum. Such barium sites are considered the most active NO_x storage sites [38].

3.3. Exposure of SO_2 under oxidising conditions in presence of water

To further investigate the effect of sulfur exposure for the $Pt/BaCO_3/Al_2O_3$ sample under more realistic conditions, the corresponding $SO_2 + O_2$ exposure was conducted in the presence of 3% water, as demonstrated in Fig. 7. Furthermore, to elucidate the effect of water during SO_2 exposure under lean conditions, IR spectra for the $Pt/BaCO_3/Al_2O_3$ sample after 30 min of $SO_2 + O_2$ exposure in the absence and presence of water are shown in Fig. 8. We note the difference in intensity scale between the right and left parts of the graph for the sake of clarity.

Generally, the spectra reveal almost the same types of adsorbed species after $SO_2 + O_2$ exposure in the absence and in presence of water. However, in the presence of water, new fea-

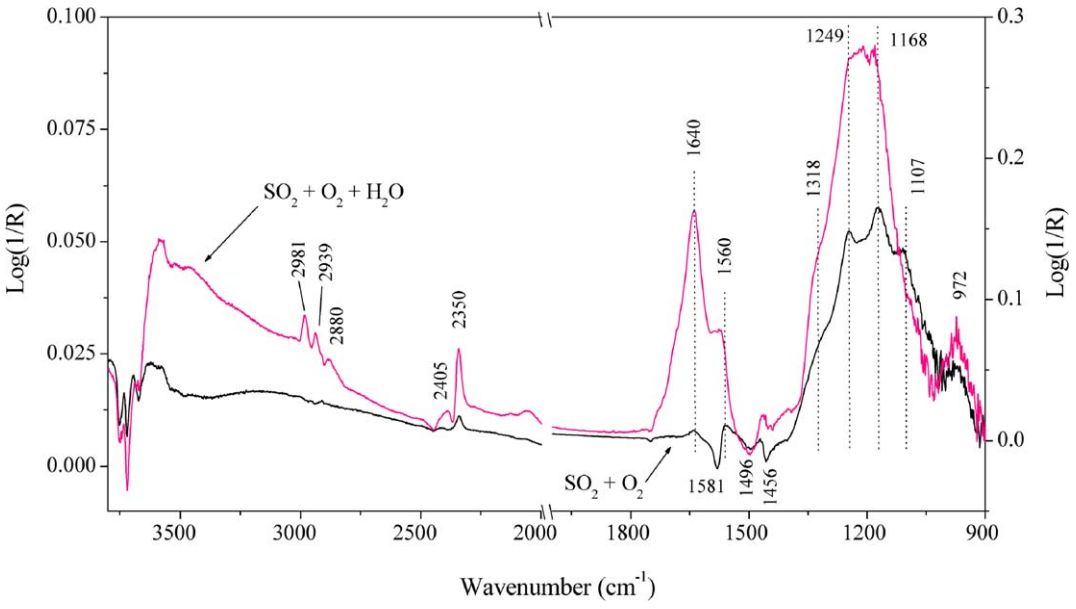

Fig. 8. DRIFT spectra for the $Pt/BaCO_3/Al_2O_3$ sample exposed to 100 ppm SO_2, 8% O_2 in Ar at 350 °C in the presence and absence of 3% H_2O after 30 min.

tures, represented by three bands at 2981, 2939, and 2880 cm^{-1} and two bands at 2405 and 2350 cm^{-1}, are observed. These peaks are most likely related to some carbon-containing species in which, as discussed previously, the carbon source likely originates from the decomposition of barium carbonate (because they appear in high-vibration frequency interval where normally no S-containing species are found [39]). However, the spectra reveal a significantly higher intensity of the peaks due to formation of bulk barium sulfate (at 1241 and 1182 cm^{-1}) and considerably lower intensity of adsorption peaks for surface barium sulfate (at around 1103 cm^{-1}). The lower intensity of surface barium sulfate could result from blockage of the barium surface by either water adsorption or hydrolysis, although the higher intensity of bulk barium sulfate suggests that water promotes the transition of surface sulfates to bulk sulfates. Another possible explanation for the greater formation of bulk barium sulfate in the presence of water could be that the water adsorbed on the barium and alumina surface enhances the oxidation of SO_2 to SO_3 over Pt, which in turn enhances the formation of bulk sulfates. Water may also promote the spillover of oxidised sulfur species from Pt to the bulk barium.

Any of the foregoing possible interpretations will likely result in considerable deterioration of NO_x storage capacity, because sulfates are more stable than their corresponding nitrates [2]. However, Elbouazzaoui et al. [31] found that even though bulk barium sulfates exist in the catalyst, complete NO_x storage recovery can be achieved under reduction with hydrogen in the presence of CO_2 and H_2O, indicating the minor effect of the bulk species on the NO_x storage process.

As for barium, the presence of water also influences the accumulation of sulfur on alumina. The formation of surface aluminum sulfate increased significantly on exposure to $SO_2 + O_2$ under humid conditions. This increase is probably due to the increased number of OH groups over alumina under humid conditions, although the interaction of SO_2 with alumina OH groups under humid conditions has been reported previously [14,15]. However, the nature of the interaction between SO_2 and the alumina OH groups has not yet been clearly elucidated. Lavalley et al. [15] suggested that SO_2 interacts with the OH group to form hydrogen sulfite ($–SO_3H$). It is worth mentioning that in the current study we did not observe the hydrogen sulfite S–H vibration band that is expected to appear at 2590 cm^{-1}. On the other hand, the SO_2 molecule may interact with the OH group via one of its oxygen atoms.

Fig. 7 also shows remarkably intense bands at 1637 and 1572 cm^{-1}. The band at 1637 cm^{-1} can be related to O–H–O bending vibrations of adsorbed water (clearly combined with a broad band between 3500 and 2500 cm^{-1}), whereas the band at 1572 cm^{-1} may be related to surface aluminum carbonate species. The increased intensity of the latter bands refers to the high ability of water to adsorb on the catalyst surface under oxidising conditions. This in turn may enhance the adsorption of the released carbon-containing species generated from barium carbonate decomposition, where a considerably higher amount of adsorbed carbonates (represented by the 1570-cm^{-1} peak) in the presence of water are observed in comparison to the absence of water.

3.4. Exposure to SO_2 under reducing conditions in the presence of water

Fig. 9 shows the collected spectra for the $Pt/BaCO_3/Al_2O_3$ sample during SO_2 exposure under reducing conditions ($SO_2 + H_2$) in the presence of 3% water. The main features in these spectra are the low intensity of the band at 1088 cm^{-1} attributed to surface barium sulfate and negative peaks at 2026, 1590, 1533, and 1370 cm^{-1}, with the latter three peaks representing the decomposition of barium carbonate and the band at 2026 cm^{-1} being related to CO adsorbed on Pt, as discussed previously. The corresponding exposure for the $BaCO_3/Al_2O_3$, Pt/Al_2O_3, and Al_2O_3 samples (not shown) shows that the fea-

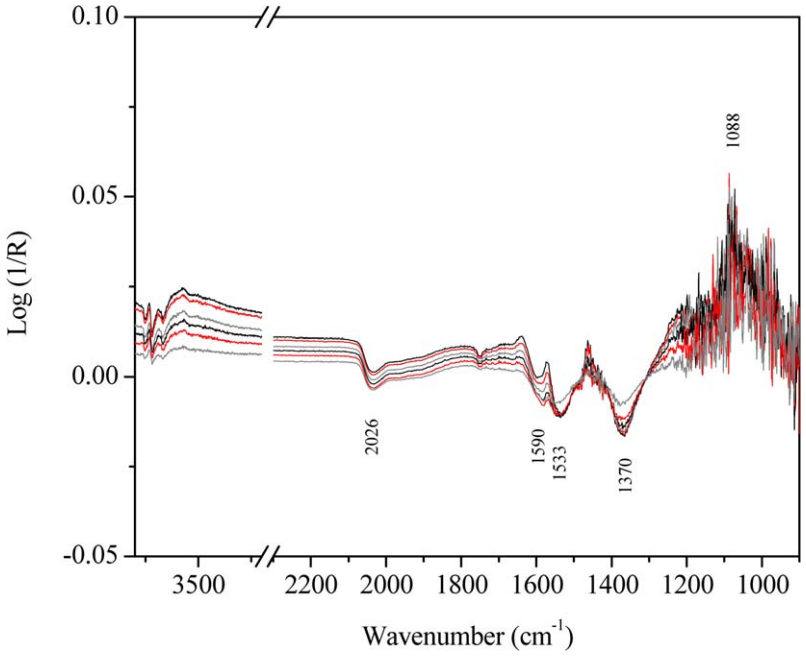

Fig. 9. DRIFT spectra for the $Pt/BaCO_3/Al_2O_3$ sample after exposure to 100 ppm SO_2, 2% H_2 and 3% H_2O in Ar at 350 °C for 5, 10, 15, 20, 25 and 30 min.

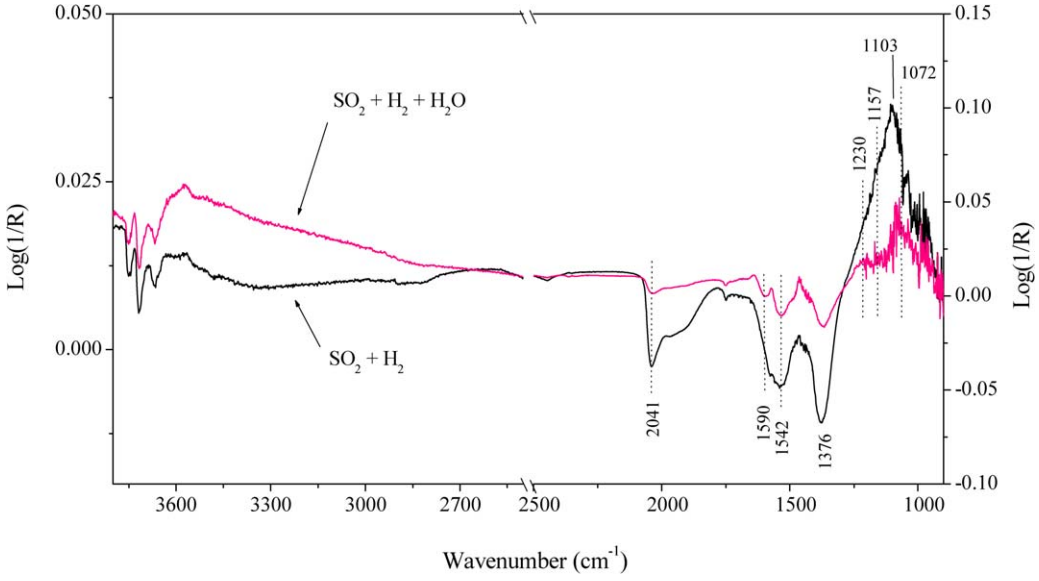

Fig. 10. DRIFT spectra for the $Pt/BaCO_3/Al_2O_3$ sample exposed to 100 ppm SO_2, 2% H_2 in Ar at 350 °C in the presence and absence of 3% H_2O after 30 min.

ture at 1088 cm^{-1} feature is observed only for the barium-containing sample (i.e., $BaCO_3/Al_2O_3$), supporting the assignment of this peak to surface barium sulfate. In addition, this sample shows a lower intensity increase for the bulk barium sulfate compared with the $Pt/BaCO_3/Al_2O_3$ sample. Unlike the corresponding experiment in the absence of water (see Fig. 4d), the presence of Pt seems to promote the formation of both surface and bulk barium sulfates under humid conditions.

The effect of water during SO_2 exposure under reducing conditions is demonstrated in Fig. 10, which compares the IR spectra in the absence and presence of water after 30 min of exposure. (Note the different intensity scales in the right and left parts of the graph.) The role of water during SO_2 exposure under reducing conditions appears to be different for the formation of sulfur species than in the corresponding experiment under oxidising conditions. A noticeable decrease in the surface barium sulfate with no formation of bulk barium sulfates is observed when water is introduced into the gas mixture. This means that barium surface sites that are considered more active NO_x storage sites can be available for NO_x storage process. However, this may be explained by the increased efficiency of hydrogen in reducing sulfur species and hydrolysing accumulated sulfide on the precious metal by water and thus in continuously regenerating these active sites, in agreement with findings of Limousy et al. [10], Liu and Anderson [5], and Elbouazzaoui et al. [31].

4. Conclusion

The exposure of $Pt/BaCO_3/Al_2O_3$ NO_x storage catalysts to SO_2 under oxidising conditions at 350 °C clearly results in the formation of surface barium sulfates that are progressively transformed to bulk sulfates. Compared with barium, alumina is (relatively) less affected by $SO_2 + O_2$ exposure and forms surface aluminum sulfates and sulfites. However, Pt does not seem to play a key role in the formation of surface and bulk barium sulfate and aluminum sulfate, where all of these species are formed on treating the $BaCO_3/Al_2O_3$ samples with $SO_2 + O_2$. On the other hand, the formation of aluminum sulfite clearly depends on the oxidation of SO_2 over the precious metal (Pt). Introducing water during lean conditions significantly influences the interaction between SO_2 and the surface of the sample. For barium, the presence of water results in a considerably lower intensity of surface barium sulfates. However, water also enhances the formation of bulk barium sulfates, probably by enhancing SO_2 oxidation over the precious metal, whereas for alumina, the presence of water increases the formation of surface aluminum sulfates while affecting sulfite formation only slightly.

SO_2 exposure under rich conditions results in decreased formation of sulfates over barium and alumina. Exposing a $SO_2 + H_2$-treated $Pt/BaCO_3/Al_2O_3$ catalysts to NO_2 results in the formation of both surface and bulk barium sulfates. This suggests that $SO_2 + H_2$ treatment may result in the accumulation of reduced sulfur-containing species on Pt and barium sites, which are oxidized by NO_2 to form surface and bulk sulfates. However, due to the high reduction efficiency of hydrogen, significant deactivation of barium and alumina storage sites with reduced sulfur species occurs under rich SO_2 exposure. These reduced sulfur species are oxidised to detectable sulfate species over barium by subsequent exposure to NO_2. Moreover, this poisoning most likely occurs on barium sites located at the platinum–barium interface, which affects the spillover of adsorbed species from precious metal to barium sites.

Acknowledgments

This work was performed at the Competence Centre for Catalysis, which is hosted by Chalmers University of Technology and is financially supported by the Swedish Energy Agency and the following member companies: Volvo Technology, Volvo Car Corporation, GM Powertrain Sweden, Perstorp Specialty Chemicals, Albemarle Catalysts, Scania CV, Haldor Topsøe, and the Swedish Space Corporation.

References

[1] W.S. Epling, L.E. Campbell, A. Yezerets, N.W. Currier, J.E. Parks, Catal. Rev. 46 (2005) 163.
[2] S. Matsumoto, CATECH 4 (2000) 102.
[3] H. Hirata, I. Hachisuka, Y. Ikeda, S. Tsuji, S.I. Matsumoto, Top. Catal. 16/17 (2001) 145.
[4] J.W. Niemantsverdriet, Spectroscopy in Catalysis, Weinheim, New York, 1993, p. 201.
[5] Z. Liu, J.A. Anderson, J. Catal. 228 (2004) 243.
[6] M.B. Mitchell, V.N. Sheinker, M.G. White, J. Phys. Chem. 100 (1996) 7550.
[7] Y. Su, M.D. Amiridis, Catal. Today 96 (2004) 31.
[8] C. Sedlmair, K. Seshan, A. Jentys, J.A. Lercher, Catal. Today 75 (2002) 413.
[9] E. Fridell, H. Persson, L. Olsson, B. Westerberg, A. Amberntsson, M. Skoglundh, Top. Catal. 16/17 (2001) 133.
[10] L. Limousy, H. Mahzoul, J.F. Brilhac, F. Garin, G. Maire, P. Gilot, Appl. Catal. B 45 (2003) 169.
[11] D. Uy, K.A. Wiegand, A.E. O'Neill, M.A. Dearth, W.H. Weber, J. Phys. Chem. B 106 (2002) 387.
[12] J.P. Breen, M. Marella, C. Pistarino, J.R.H. Ross, Catal. Lett. 80 (2002) 123.
[13] S. Poulston, R.R. Rajaram, Catal. Today 81 (2003) 603.
[14] C.C. Chang, J. Catal. 53 (1978) 374.
[15] J.C. Lavalley, A. Janin, J. Preud'homme, React. Kinet. Catal. Lett. 18 (1981) 85.
[16] A. Amberntsson, M. Skoglundh, S. Ljungström, E. Fridell, J. Catal. 217 (2003) 253.
[17] K. Yamazaki, T. Suzuki, N. Takahashi, K. Yokota, M. Sugiura, Appl. Catal. B 30 (2001) 459.
[18] P.T. Fanson, M.R. Horton, W.N. Delgass, J. Lauterbach, Appl. Catal. B 46 (2003) 393.
[19] J. Dawody, M. Skoglundh, L. Olsson, E. Fridell, J. Catal. 234 (2005) 206.
[20] F. Rohr, S.D. Peter, E. Lox, M. Kögel, A. Sassi, L. Juste, C. Rigaudeau, G. Belot, P. Gélin, M. Primet, Appl. Catal. B 56 (2005) 201.
[21] H. Abdulhamid, E. Fridell, M. Skoglundh, Appl. Catal. B 62 (2005) 319.
[22] A. Amberntsson, B. Westerberg, P. Engström, E. Fridell, M. Skoglundh, Stud. Surf. Sci. Catal. 126 (1999) 317.
[23] H. Knözinger, P. Ratnasamy, Catal. Rev. Sci. Eng. 17 (1978) 31.
[24] F.J. Garcia, S. Guerrero, E.E. Wolf, J.T. Miller, A.J. Kropf, J. Catal. 233 (2005) 372.
[25] H. Mahzoul, L. Limousy, J.F. Brilhac, P. Gilot, J. Anal. Appl Pyrol. 56 (2000) 179.
[26] O. Saur, M. Bensitel, A.B.M. Saad, J.C. Lavalley, C.P. Tripp, B.A. Morrow, J. Catal. 99 (1986) 104.
[27] T. Yu, H. Shaw, Appl. Catal. B 18 (1998) 105.
[28] P.-A. Carlsson, L. Osterlund, P. Thormahlen, A. Palmqvist, E. Fridell, J. Jansson, M. Skoglundh, J. Catal. 226 (2004) 422.
[29] M. Primet, J.M. Basset, M.V. Mathieu, M. Prettre, J. Catal. 29 (1973) 213.
[30] R.M. Silverstein, G.C. Bassler, T.C. Morrill, Spectrometric Identification of Organic Compounds, Wiley, New York, 1991, p. 97.
[31] S. Elbouazzaoui, E.C. Corbos, X. Courtois, P. Marecot, D. Duprez, Appl. Catal. B 61 (2005) 236.
[32] H.H. Eysel, H. Siebert, G. Agiorgitis, Z. Naturforsch. 24 (1969) 932.
[33] C. Yanxin, J. Yi, L. Wenzhao, J. Rongchao, T. Shaozhen, H. Wenbin, Catal. Today 50 (1999) 39.
[34] Y. Wang, A.B. Mohammed Saad, O. Saur, J.C. Lavalley, B.A. Morrow, Appl. Catal. B 16 (1998) 279.
[35] C. Sedlmair, K. Seshan, A. Jentys, J.A. Lercher, J. Catal. 214 (2003) 308.
[36] F. Prinetto, G. Ghiotti, I. Nova, L. Castold, L. Lietti, E. Tronconib, P. Forzatti, Phys. Chem. Chem. Phys. 5 (2003) 4428.
[37] L. Olsson, H. Persson, E. Fridell, M. Skoglundh, B. Andersson, J. Phys. Chem. B 105 (2001) 6895.
[38] I. Nova, L. Castoldi, L. Lietti, E. Tronconi, P. Forzatti, F. Prinetto, G. Ghiotti, J. Catal 222 (2004) 377.
[39] K. Nakamoto, Infrared and Raman Spectra of Inorganic and Coordination Compounds, Part A: Theory and Applications in Inorganic Chemistry, Wiley, New York, 1997.